Power Absorption and Temperature Elevations Induced in the Human Head by a Dual-Band Monopole-Helix Antenna Phone

Paolo Bernardi, *Fellow, IEEE*, Marta Cavagnaro, Stefano Pisa, *Member, IEEE*, and Emanuele Piuzzi

***Abstract*—A numerically efficient way to evaluate specific absorption rate (SAR) deposition and temperature elevation inside the head of a user of a cellular phone equipped with a dual-band monopole-helix antenna is proposed. The considered antenna operates at both frequencies (900 and 1800 MHz) employed in global system for mobile communication. The results obtained show that, for a given radiated power, although the maximum SAR value as averaged over 1 g in the brain is higher at 900 MHz than at 1800 MHz, the maximum temperature increase in the brain is higher at 1800 MHz. However, taking into account that the average power levels radiated at the two operating frequencies are different (250 mW at 900 MHz and 125 mW at 1800 MHz), higher temperature elevations are obtained at 900 MHz. In this last case, the temperature increases are of the order of 0.2 °C in the ear, and less than 0.1 °C in the external brain region close to the phone. When the heating effect due to the contact of the ear and cheek with the phone is also taken into account, it is found that the predominant heating effect in the ear, able to cause temperature increases as high as 1.5 °C, is the one due to the phone contact, while SAR deposition plays a significant role only in the heating of the external brain region.**

***Index Terms*—Biological effects of electromagnetic radiation, dosimetry, electromagnetic heating, FDTD methods, land mobile radio cellular systems, temperature.**

I. Introduction

THE ever-rising diffusion of cellular phones has determined an increased concern for possible adverse health effects due to the field emitted by the handheld terminals. The evaluation of the power absorbed in the user's head is a key task, both for design and compliance testing of cellular phones, that can be efficiently performed numerically. At present, among the numerical techniques, the most often applied in the presence of highly nonhomogeneous structures, like the human head, is the finite-difference time-domain (FDTD) method, thanks to its efficiency and ease of implementation [1]–[3]. Generally, in FDTD studies, the phone radiating element is simulated as a half-wavelength dipole, a quarter-wavelength monopole, or a whip antenna [4]–[10]. All these antenna models, and the last two in particular, can be used as approximate (quarter-wavelength monopole) or realistic (whip antenna) models of pullout antennas, which were equipping, until some time ago, almost all cellular handsets. Today, however, the need for more and more compact terminals and for dual-band operation has arisen, and new antenna types are being used; one of the most diffused being the helical antenna. Therefore, the solution of the problem of the electromagnetic (EM) dosimetry for a human head exposed to a handheld terminal equipped with a helical antenna becomes of primary importance. While monopole and planar antennas can be easily implemented inside an FDTD code, as confirmed by the many FDTD studies available in literature, modeling of a helix can become a rather difficult task. In fact, only rather large structures have been studied employing a pure FDTD scheme [11], while for smaller structures, either equivalent sources [12] or a hybrid method of moments (MoM)/FDTD technique [13], [14] have been employed. Since all these techniques show some problems and drawbacks, the applicability of a pure FDTD approach, properly modified to allow the use of a graded mesh, has been investigated [15], [16].

Numerical dosimetry applied to the problem of human-head exposure to fields radiated by cellular phones exhaustively answered many questions, but some problems are still open. In particular, one of them is the evaluation of induced temperature increases in the user's head, which can be directly compared with the thresholds for the induction of known adverse thermal effects in the human head. Unfortunately, if much has been done in the field of numerical dosimetry, only a few papers are available addressing the EM-field/human-body interaction problem also from a thermal point-of-view [17]–[19]. In particular, in all these studies, power deposition and temperature increase in the head of a cellular phone user have been evaluated only for cellular phones equipped with linear or planar antennas. Moreover, the above-cited studies have mainly considered the heating effect due to the specific absorption rate (SAR). However, in practical situations, two more causes for temperature increase are present. The first one is the contact between the phone case and the user's head (in particular, ear and cheek) that blocks the convective heat exchange between the skin layers and air, causing temperature rises in the tissues around the contact zone. Obviously, this heating is totally independent from the radiated power and, indeed, it can also be observed for a wireline phone. The second additional cause for temperature increase is the heating of the phone itself, due to the power dissipated in the circuitry and, in particular, in the power amplifier; this heating is transmitted to the head tissues via thermal conduction.

In this paper, the problem of SAR deposition and temperature elevation inside the head of a user of a cellular phone equipped with a dual-band monopole-helix antenna is numerically solved

Manuscript received March 30, 2001; revised July 29, 2001.

The authors are with the Department of Electronic Engineering, University "La Sapienza" of Rome, 00184 Rome, Italy (e-mail: bernardi@die.ing.uniroma1.it).

Publisher Item Identifier S 0018-9480(01)10432-1.

0018–9480/01$10.00 © 2001 IEEE

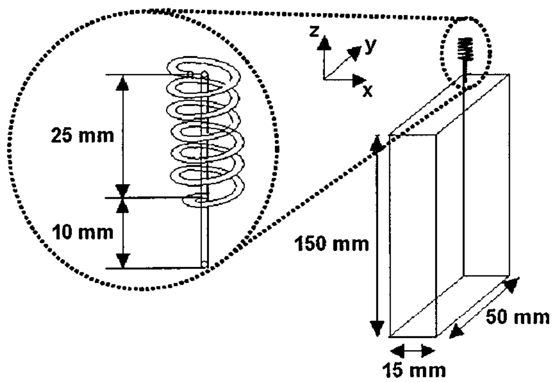

Fig. 1. Cellular phone model (the plastic shell enclosing the metal case is not shown).

by using a graded-mesh FDTD approach for the solution of the dosimetric problem, and a finite-difference implementation of the bio-heat equation (BHE) for the solution of the thermal problem. In particular, the thermal study aims at investigating the effect on induced temperature elevations not only of SAR, but also of phone contact and power dissipation in the circuitry.

II. Methods and Models

The power deposition in a human-head model due to a cellular phone equipped with a dual-band monopole-helix antenna has been computed by using the FDTD numerical technique [1]–[3] with a graded mesh [15], [16].

The considered head model has been obtained from a tissue-classified version of the "Visible Human" image set developed at Brooks Air Force Base Laboratories, Brooks AFB, TX [20]. The model has a 3-mm resolution and discriminates 19 different types of tissues/organs. For the electrical characterization of the tissues at the considered frequencies, Gabriel's data [21], [22] have been used.[1]

A cellular phone equipped with a recently proposed dual-band monopole-helix antenna [23] has been considered. This antenna is constituted of a helix mounted on a straight metal connection and of a monopole placed inside the helix (see Fig. 1). The diameter, pitch, and length of the helix are 5.5, 4.4, and 27 mm, respectively, and the straight metal connection is 10-mm long. All dimensions are chosen to achieve resonance at 900 MHz. The monopole is 25-mm long and, together with the straight metal connection, is tuned to operate at 1800 MHz. The wire radius is equal to 0.8 mm. The helix is mounted on the right-hand corner of a metallic case, in the far end with respect to the side of the earphone. The phone metal case is $15 \times 50 \times 150$ mm wide, and it is enclosed by a 3-mm-thick lossless dielectric shell ($\varepsilon_r = 2.7$).

In the FDTD analysis of the considered phone, the section of the wire has been modeled, within the fine-resolution region of the graded mesh, with a five-cell cross [16]. The size of the cells in the high-resolution region has been chosen equal to 0.55 mm. The largest cell size has been chosen equal to 3 mm and the grading factor equal to two. The antenna has been fed, at the connection between the metallic case and straight wire, with a Gaussian pulse, thus exploiting the capability of FDTD to perform a wide-band analysis of the structure. The simulation has been interrupted when the current at the antenna feed point was reduced at least of three orders of magnitude with respect to the peak value.

To evaluate the temperature distribution $T = T(\boldsymbol{r}, t)$ inside the user's head, a finite-difference formulation of the BHE [19] has been used. This equation describes the different ways through which heat is transferred, produced, or removed inside the tissues, and, precisely: heat transfer through internal conduction, metabolic heat production, exogenous heat deposition, and heat-exchange mechanism due to capillary blood perfusion. The BHE can be adopted to study the temperature increase induced inside subjects exposed to EM fields, after a dosimetric analysis has been performed. In fact, the power absorption induced by the EM-field exposure can be represented, inside the BHE, as an exogenous heat deposition term that is responsible for the alteration in temperature profiles inside the biological tissues with respect to the unexposed situation. This term, which represents a volumetric heat deposition, can be directly derived from the SAR distribution, simply multiplying the SAR by the tissue mass density ρ [19].

The values assumed for the thermal parameters of the different head tissues have been directly taken or extrapolated from existing literature and can be found in [19].

III. Results

A. Phone Model Validation

First of all, a simulation has been performed to study the free-space radiating properties of the phone, in order to assess graded-mesh FDTD accuracy. To this end, the results of the FDTD analysis have been compared with those obtained analyzing the same phone with the MoM by using the freely available numerical electromagnetics code (NEC) program [24]. The choice of validating the phone model in a free-space situation, instead of considering exposure of a user's head, is justified by the fact that the NEC implementation of the MoM is able to handle only metallic objects. For this reason the 3-mm-thick dielectric shell that encloses the metallic case of the real phone has been neglected. In MoM simulations, the phone box has been modeled employing a wire-grid model with a spatial step of about 7.5 mm, reduced to about 2.5 mm in the zone where the straight wire connecting the helix to the box is present. The helix has been modeled employing 120 segments (i.e., 20 segments per turn).

Since it has been demonstrated that the SAR in an exposed head is mainly related to the near H-field produced by the cellular phone [25], this field, computed at the two frequencies of operation by using the graded-mesh FDTD approach, has been compared with the one evaluated by the MoM. In particular, in the FDTD simulation, the magnetic-field amplitude has been evaluated through a discrete Fourier transform of the H-field components. Comparison of the normalized distribution of the H-field on the plane parallel to the x–z-plane of Fig. 1 containing the straight metal connection has shown optimum agreement between the FDTD and MoM.

[1][Online]. Available: http://www.fcc.gov/fcc-bin/dielec.sh

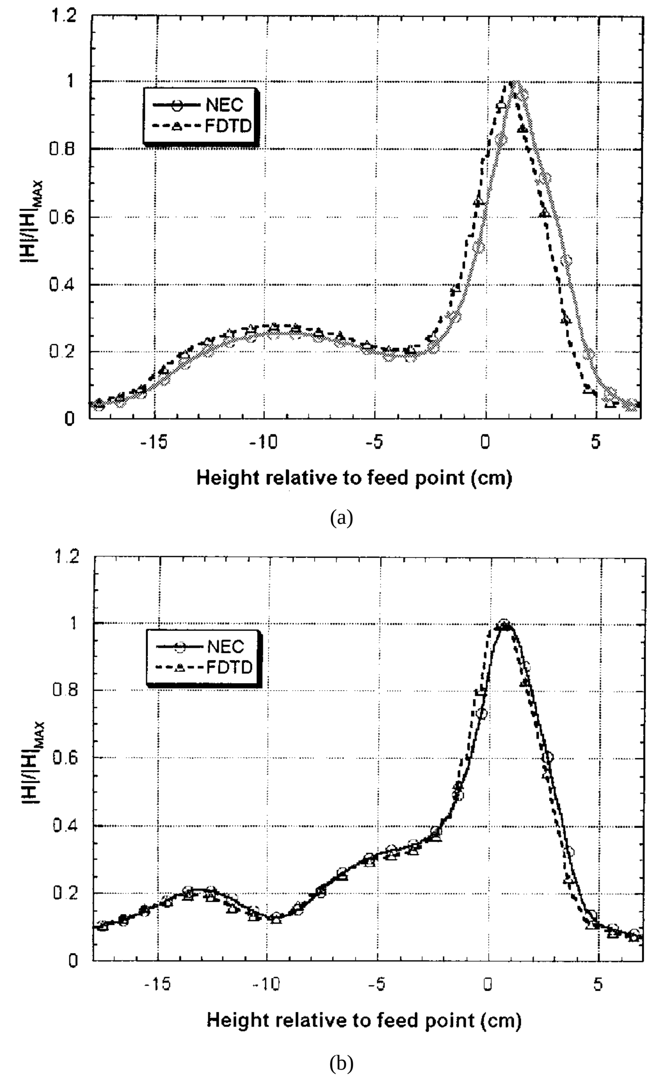

Fig. 2. H-field normalized amplitude along a vertical line 1 cm far from the straight metal connection in the -x-direction. (a) $f = 900$ MHz. (b) $f = 1800$ MHz.

As an example, the normalized magnitude of the H-field computed, employing the FDTD and MoM, on a vertical line lying on the above-described plane, and placed at a distance of approximately 1 cm from the metal connection, on the left-hand side of the connection itself, is reported in Fig. 2. This figure shows the optimum agreement obtained between the two techniques.

The far-field radiating properties of the phone have been also analyzed. In particular, the radiation pattern at the two operating frequencies has been evaluated employing both the FDTD and MoM. In the FDTD simulation, the radiation pattern has been evaluated through a discrete Fourier transform of the near-field components and by applying a near-to-far-field transformation. A cut of the radiation pattern on the z–y-plane of Fig. 1, obtained by using both the graded-mesh FDTD and MoM, and normalized to the maximum gain, is reported in Fig. 3 for the two operating frequencies. Fig. 3 shows that the antenna operates in normal mode with a down tilting of about 30°. An excellent agreement is observed between the graded-mesh FDTD and MoM.

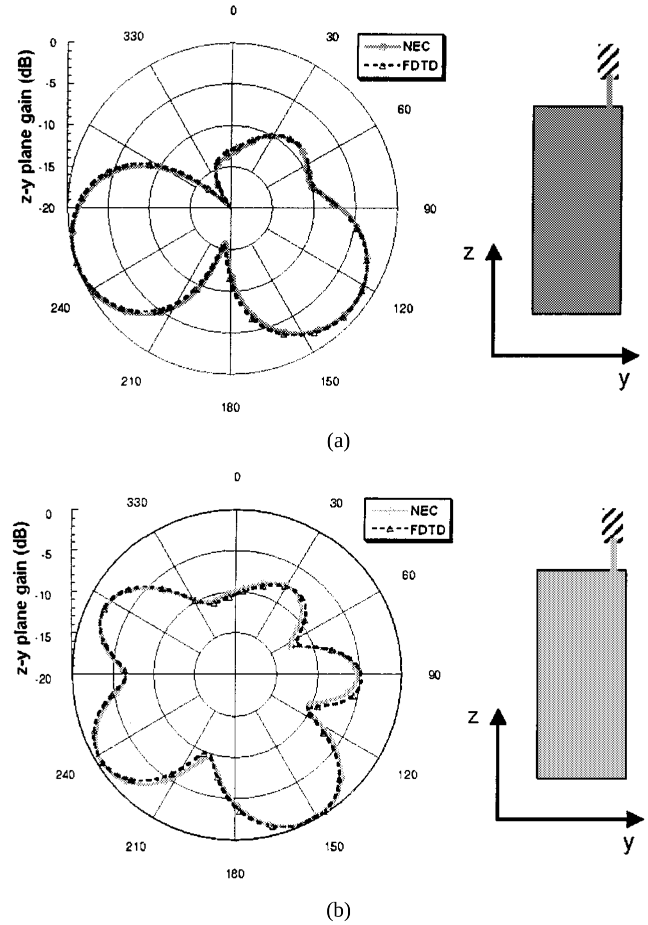

Fig. 3. Normalized free-space radiation pattern on the z–y-plane. (a) $f = 900$ MHz. (b) $f = 1800$ MHz.

The comparisons between the graded-mesh FDTD and MoM, concerning both near- and far-field analysis, show the capability of the graded-mesh FDTD to correctly characterize the fine structure of the realistic monopole-helix antenna considered.

B. SAR and Induced Heating: Differences Between 900 and 1800 MHz

The interaction between the considered phone and human-head models has been studied with a reference radiated power of 1 W, in order to highlight the differences in the SAR and induced heating due to the different operating frequencies. In this initial study, the phone has been kept in a vertical position, with the ear piece aligned with the auditory canal and the phone case in direct contact with the ear. A discrete Fourier transform of the electric field inside the head has been used to evaluate the field amplitude, from which the SAR distribution has been derived. Fig. 4 shows, for the chosen radiated power of 1 W, the SAR distributions evaluated on the coronal vertical plane passing through the point where the maximum SAR is located. This figure evidences the higher penetration depth at 900 MHz, and the higher superficial SAR values obtained at 1800 MHz. In particular, at the frequency of 900 MHz about 800 mW are absorbed inside the head, while the maximum SAR values as averaged over 1 and 10 g

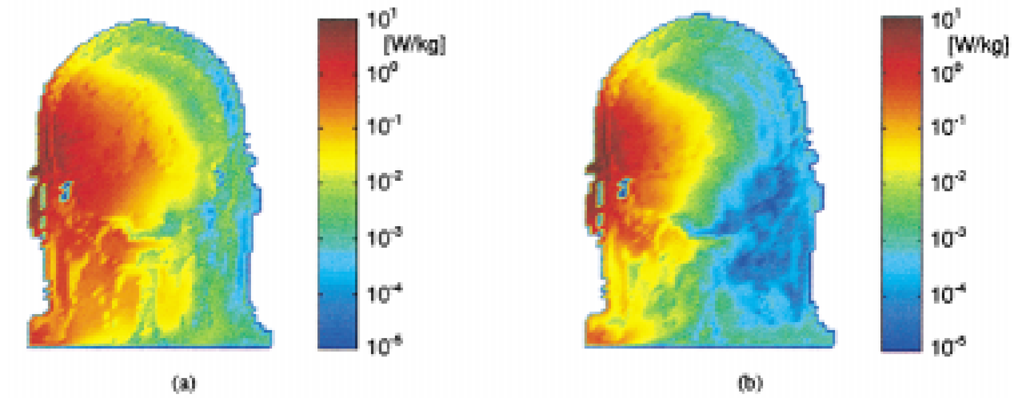

Fig. 4. SAR distribution for a radiated power of 1 W. (a) $f = 900$ MHz. (b) $f = 1800$ MHz.

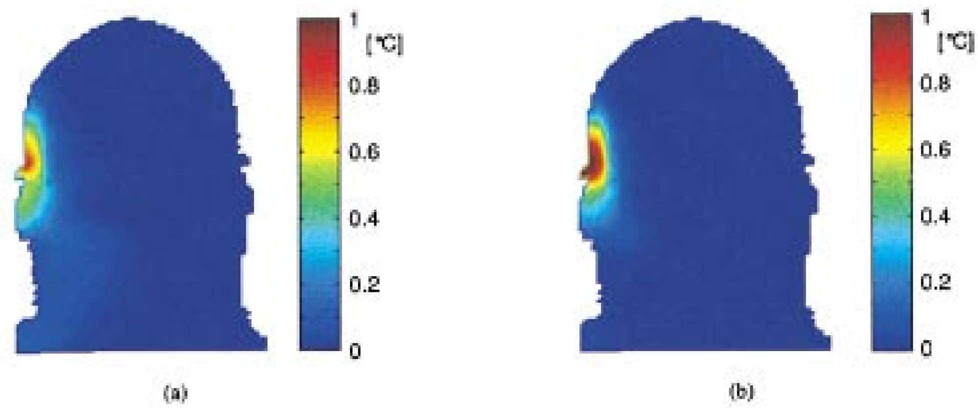

Fig. 5. Temperature increase distribution for a radiated power of 1 W. (a) $f = 900$ MHz. (b) $f = 1800$ MHz.

in the head (SAR_{1g} and SAR_{10g}), and over 1 g in the brain ($\mathrm{SAR}_{1gBRAIN}$) are equal to 8.24, 4.77, and 1.29 W/kg, respectively. At the frequency of 1800 MHz, one-half of the radiated power (i.e., 500 mW) is absorbed inside the head, while the SAR_{1g}, SAR_{10g}, and $\mathrm{SAR}_{1gBRAIN}$ values are equal to 14.46, 6.93, and 0.93 W/kg, respectively. In conclusion, at 1800 MHz, the maximum SAR values averaged over 1 and 10 g increase with respect to the 900-MHz situation, while the SAR in the brain and the total power absorbed in the head reduce. Similar results have been obtained by Dimbylow and Mann [26] and Gandhi *et al.* [27].

With reference to the steady-state temperature increase ($\Delta\mathrm{T}$), Fig. 5 shows the $\Delta\mathrm{T}$ distributions at 900 and 1800 MHz on the same plane of Fig. 4. From Fig. 5, it can be noted that the maximum temperature rise ($\Delta\mathrm{T}_{\max}$) is always obtained in the ear. A comparison between the two operation frequencies reveals that, at 1800 MHz, higher values are obtained with respect to the 900-MHz situation, as expected from the SAR results. In particular, the $\Delta\mathrm{T}_{\max}$ obtained in the ear region are equal to 0.93 °C and 1.28 °C at 900 and 1800 MHz, respectively. A temperature rise of 0.26 °C (900 MHz) and 0.31 °C (1800 MHz) is present in the external part of the brain close to the phone ($\Delta\mathrm{T}_{\max\,\mathrm{BRAIN}}$). It is worth noting that, in the brain, the $\Delta\mathrm{T}_{\mathrm{MAX}}$ is higher at 1800 MHz with respect to the 900 MHz exposure, thus reversing the $\mathrm{SAR}_{1gBRAIN}$ behavior.

In order to better understand the differences in power absorption and induced temperature increases at the two operating frequencies, Fig. 6 shows the profiles of the free-space squared magnetic-field amplitude, SAR, and induced temperature elevations along a line parallel to the x-axis of Fig. 1 and passing through the point of the ear where the maximum SAR value is obtained. The H-field profile [see Fig. 6(a)] shows that the magnetic field produced by the phone at 1800 MHz is higher than that at 900 MHz, at least in the region near the case where the ear will be located, and that it decreases more quickly than at 900 MHz. The most interesting information, however, can be drawn from the SAR and $\Delta\mathrm{T}$ profiles [see Fig. 6(b) and (c)]. In order to correctly analyze these profiles, it must be noted that, along the examined line, the brain cortex begins at a distance from the case of approximately 2.5 cm. Fig. 6(b) shows that, at 1800 MHz, due to the higher magnetic field and to the higher tissue conductivity, higher SAR values are obtained in the first skin layers, as compared to those computed at 900 MHz. However, the losses within the biological tissues, being higher at 1800 MHz, cause the SAR profile to attenuate more rapidly. In particular, the figure shows that SAR curves computed at the two frequencies intersect at a distance from the case of about 2.5 cm,

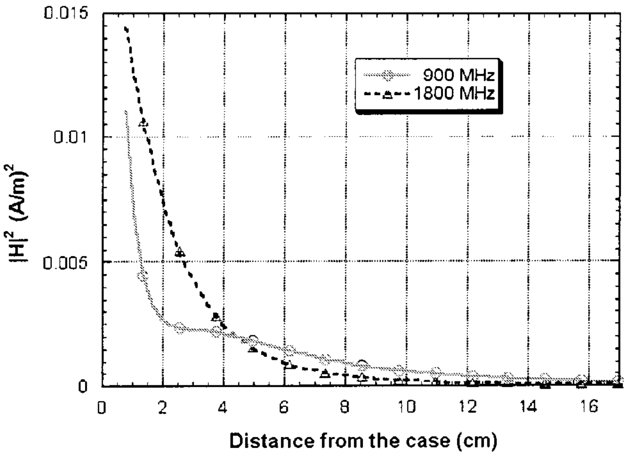

(a)

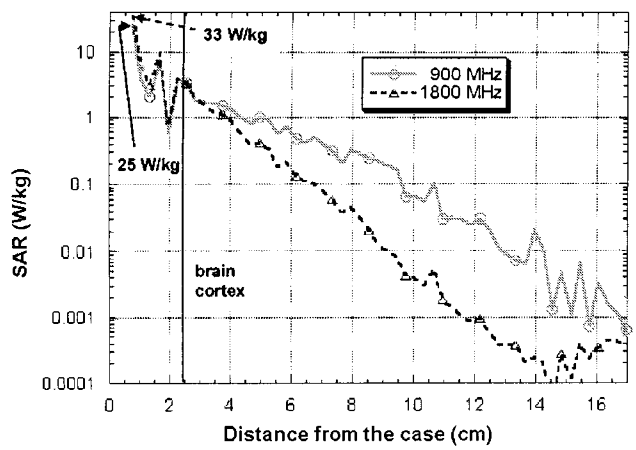

(b)

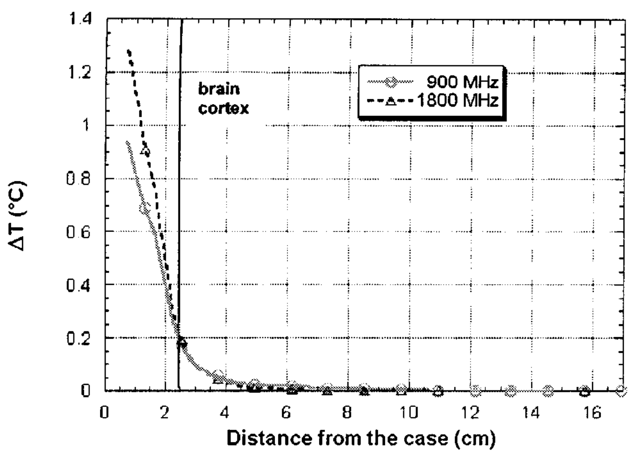

(c)

Fig. 6. Penetration curves for a radiated power of 1 W. (a) Squared H-field amplitude. (b) SAR. (c) ΔT.

just below the brain surface. As the cube used for computing $\mathrm{SAR}_{1\mathrm{gBRAIN}}$ extends 1 cm in depth from the brain surface, a lower $\mathrm{SAR}_{1\mathrm{gBRAIN}}$ is obtained at 1800 MHz. Temperature increase profiles, reported in Fig. 6(c), show a penetration profile having a shape that is much smoother than that of SAR. Also in this case, it can be noted that the profiles computed at the two frequencies intersect in a point located just below the brain surface, thus explaining the reason why $\Delta T_{\max \mathrm{BRAIN}}$ is slightly higher at 1800 MHz than at 900 MHz.

C. SAR and Induced Heating Under Realistic Use Conditions

In the previous subsection, temperature elevations induced in the user's head have been evaluated, neglecting heating effects due to the phone contact and power dissipation in the circuitry, and considering a reference radiated power of 1 W, which does not correspond to the global system for mobile communication (GSM) system standard [28].

The aim here is to investigate the temperature increases induced under realistic use conditions. This is accomplished considering also the heating effects due to the phone contact and dissipation, and scaling the average radiated powers to those typical of the GSM system, namely, 250 mW at 900 MHz, and 125 mW at 1800 MHz. Obviously, in order to correctly characterize the effect due to the phone contact, it is necessary to refer to a realistic position of the phone, ensuring an extended contact area between the phone case and user's cheek. There-

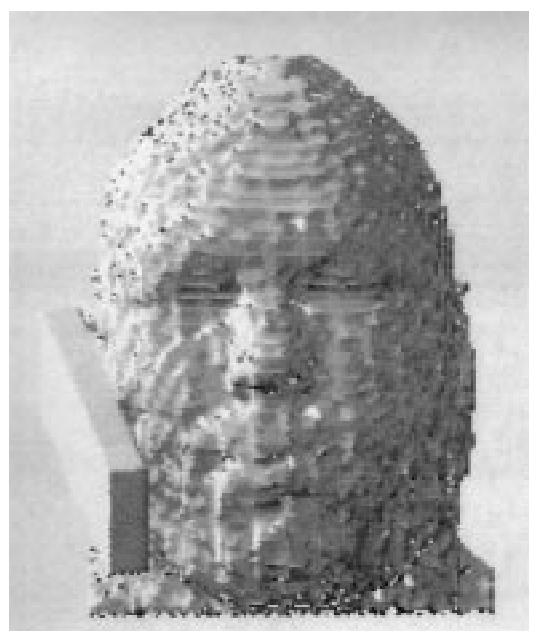

Fig. 7. Cellular phone held in a realistic "cheek" position.

TABLE I
SAR IN THE HEAD OF A USER OF A PHONE EQUIPPED WITH A DUAL-BAND MONOPOLE-HELIX ANTENNA. AVERAGE RADIATED POWER: 250 mW AT 900 MHz AND 125 mW AT 1800 MHz

Frequency [MHz]	Position	SAR_{1g} [W/kg]	SAR_{10g} [W/kg]	$SAR_{1gBRAIN}$ [W/kg]
900	Vertical	2.06	1.19	0.32
	"Cheek"	1.65	0.91	0.13
1800	Vertical	1.81	0.87	0.12
	"Cheek"	1.08	0.56	0.06

fore, together with the previously examined vertical position, a double-tilting position has been also considered for the phone. A three-dimensional view of the phone–head geometry, with the phone in double tilting or "cheek" position, is depicted in Fig. 7. In the graded-mesh FDTD code, the double tilting has been obtained leaving the phone in a vertical position and rotating the head first forward by an angle of 60°, and then applying a further rotation of 12° toward the phone around the head vertical axis. In this manner, the microphone has been aligned with the user's mouth, and the phone case has been brought in close contact with the cheek.

The $\mathrm{SAR}_{1\mathrm{g}}$, $\mathrm{SAR}_{10\mathrm{g}}$, and $\mathrm{SAR}_{1\mathrm{gBRAIN}}$ values computed at the two frequencies, with the average radiated power set to the GSM standard maximum level, are reported in Table I, both for the phone kept in the vertical position and in the "cheek" position. The table shows that, due to the lower radiated power, SAR values obtained at 1800 MHz under realistic use conditions are always lower than those computed at 900 MHz. As concerns the effect of moving the phone from the vertical position to the "cheek" position, it can be noted that this change of position causes a reduction of all SAR values. It must be noted that bringing the phone to the "cheek" position not only alters the SAR values, but also causes a marked variation in the characteristics of the SAR distribution. In particular, the highest SAR values tend to move to the bottom part of the ear, strictly pressed against the phone, and the $\mathrm{SAR}_{1\mathrm{gBRAIN}}$ shows a decrease, which is more relevant than the one appearing on $\mathrm{SAR}_{1\mathrm{g}}$ and $\mathrm{SAR}_{10\mathrm{g}}$, due to the greater distance of the antenna from the brain. Comparing SAR values reported in Table I with limits issued by exposure guidelines [29]–[32], it is found that the limit of 2.0 W/kg averaged over 10 g of tissue [29], [30] is always respected, while the more stringent limit of 1.6 W/kg averaged over 1 g [31], [32] is always exceeded, except when the phone is kept in a double-tilting position and operates at 1800 MHz.

After studying power absorption, the temperature elevations induced under realistic conditions have been evaluated, assessing the influence of the different heating causes considered. To this end, first of all, a study has been performed to evaluate heating induced by the SAR alone, both for the vertical-oriented and "cheek" phone positions. Heating induced inside the head by the contact between the phone and the ear, and by the dissipation in the power amplifier, neglecting SAR, has also been considered. In this case, only the "cheek" position has been analyzed because it is the only one that ensures a significant contact area between the phone and head surface. The dissipation in the power amplifier has been simulated adding a power deposition of 250 mW at 900 MHz and 125 mW at 1800 MHz uniformly distributed inside the upper part of the phone, supposing a 50% efficiency. As concerns thermal conductivity for the plastic shell and metal case, values of 0.013 and 1.0 W/(m°C), respectively, have been used [33]. It must be observed that the value chosen for metal is much lower than the real thermal conductivity of a metallic material (e.g., copper) because it has been assumed that, in the real phone, only part of the case is constituted by metal, the remaining part being filled by air or printed circuit boards. The used value, therefore, is a sort of average thermal conductivity for the phone case. Finally, after having considered the single effects, due to SAR, phone contact, and power dissipation in the amplifier separately, these effects have been considered simultaneously, in order to obtain the complete thermal elevation.

TABLE II
TEMPERATURE ELEVATIONS INDUCED IN THE USER'S HEAD, AFTER 15 min, BY A PHONE EQUIPPED WITH A DUAL-BAND MONOPOLE-HELIX ANTENNA. AVERAGE RADIATED POWER: 250 mW AT 900 MHz AND 125 mW AT 1800 MHz

Freq. [MHz]	Position	Heating cause	ΔT_{max} [°C]	$\Delta T_{maxBRAIN}$ [°C]
900	Vertical	SAR	0.221	0.061
	"Cheek"	SAR	0.136	0.023*
		Contact	1.543	0.012**
		Contact + power dissipation	1.544	0.012**
		Contact + power dissip. + SAR	1.581	0.023*
1800	Vertical	SAR	0.155	0.036
	"Cheek"	SAR	0.085	0.011*
		Contact	1.543	0.012**
		Contact + power dissipation	1.543	0.012**
		Contact + power dissip. + SAR	1.549	0.012**

* $\Delta T_{maxBRAIN}$ located in the upper external brain region
** $\Delta T_{maxBRAIN}$ located in the lower external brain region

All thermal simulations have been performed assuming the air temperature is equal to 24 °C. Moreover, in order to resemble as close as possible a realistic situation, temperature elevations have been computed for a time interval of 15 min, corresponding to the duration of a rather long phone call. This means that the computed temperature increases refer to a situation in which steady state has not been reached as yet, although temperature elevations evaluated after 15 min are expected to be very close to the steady-state value [19].

The maximum temperature elevations obtained, after 15 min of phone call, in the ear and brain of the user's head, considering the different heating causes previously described, are reported in Table II for the two operating frequencies.

Analysis of Table II reveals some interesting aspects. First of all, it is possible to observe that the temperature elevation induced inside the brain by SAR alone is below 0.1 °C, especially when the phone is kept in the "cheek" position, which, as al-

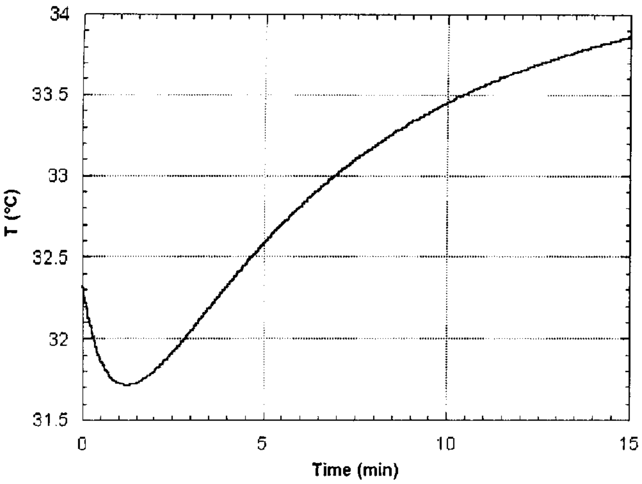

Fig. 8. Time evolution of the temperature in a point of the ear in direct contact with a nonradiating phone.

ready commented, determines a marked reduction in power deposition inside the brain.

Table II also shows that the mere contact of the cellular phone with the ear and cheek, even in a standby condition, in which no power is radiated and no power is internally dissipated, causes temperature elevations in the ear reaching 1.5 °C, due to the highly insulating properties assumed for the phone plastic shell. A negligible maximum temperature elevation of about 0.01 °C, instead, is caused in the external brain region. It is also possible to observe that, if the further contribution due to power dissipation in the amplifier is added, induced temperature elevations are not significantly altered. Finally, it is worth noting the effect that the phone contact has on the temperature evolution in the ear region (see Fig. 8). The phone is initially at ambient temperature (24 °C), which is usually lower than the ear temperature; therefore, when the phone is put in contact with the ear, it determines a quick decrease in the ear temperature. Soon after, however, the heat supplied by blood and the one coming from the neighboring tissues stops this decrease, and temperature starts to elevate, going beyond the initial value, due to the suppressed convective exchange with air.

Coming, finally, to the case when all heating effects are considered simultaneously, the following observations can be done. The maximum temperature elevation in the ear is almost entirely due to the contact effect, with only a very slight contribution due to the SAR deposition in the ear region. The situation, instead, is completely different in the brain region. In fact, it must be observed that the two heating effects, due to the SAR and phone contact, tend to heat different parts of the brain, with the contact effect heating the lower external brain region, and the SAR heating the upper external brain region. Therefore, these two heating effects are not additive in the brain, and when they are simultaneously present, as opposed to the case when only one is considered, the result is that the portion of the brain affected by heating becomes larger. The peak temperature increase in the brain is, therefore, governed by the most important between the two heating causes. At 900 MHz, the most relevant effect is the one due to the SAR, while at 1800 MHz, due to the lower radiated power, the two heating effects are comparable.

IV. Conclusions

SAR distributions and temperature increases have been evaluated in a head model exposed to the field radiated by a cellular phone, equipped with a monopole-helix antenna operating at 900 and 1800 MHz. The obtained results confirm the importance of performing a thermal analysis together with the dosimetric one. At the same levels of radiated power, operation at 1800 MHz results in higher SAR and temperature increases with respect to 900 MHz. When the powers really radiated at the two frequencies by GSM phones are considered, however, it is found that temperature elevations induced in the external brain region at 1800 MHz are halved, as compared to those induced by 900-MHz operation. In any case, induced temperature elevations, in all the examined conditions, never exceed 0.1 °C in the brain region. This value is well below the threshold for the induction of adverse thermal effects to the neurons [34]. It is worth noting that the reported temperature elevations have been computed assuming that the phone is operating at the maximum power levels permitted by the GSM standard. In real-life operation, however, thanks to power control and discontinuous transmission (DTX), it is expected that the radiated power levels are lower than the maximum ones, thus lowering induced temperature increases [35]. Finally, it is important to evidence that the simulations performed to study the effect of the phone contact on temperature elevations have shown that, indeed, the most relevant heating cause in the ear is the one due to the suppression of convective heat exchange from the ear and cheek to the air, due to the contact with the phone.

References

[1] K. S. Kunz and R. J. Luebbers, *The Finite Difference Time Domain Method for Electromagnetics*. Boca Raton, FL: CRC Press, 1993.

[2] A. Taflove, *Computational Electrodynamics: The Finite-Difference Time-Domain Method*. Norwood, MA: Artech House, 1995.

[3] ——, *Advances in Computational Electrodynamics: The Finite-Difference Time-Domain Method*. Norwood, MA: Artech House, 1998.

[4] J. Toftgard, S. N. Hornsleth, and J. B. Andersen, "Effects on portable antennas of the presence of a person," *IEEE Trans. Antennas Propagat.*, vol. 41, pp. 739–746, June 1993.

[5] P. J. Dimbylow and S. M. Mann, "SAR calculations in an anatomically realistic model of the head for mobile communication transceivers at 900 MHz and 1.8 GHz," *Phys. Med. Biol.*, vol. 39, pp. 1537–1553, 1994.

[6] P. Bernardi, M. Cavagnaro, and S. Pisa, "Evaluation of the SAR distribution in the human head for cellular phones used in a partially closed environment," *IEEE Trans. Electromagn. Compat.*, vol. 38, pp. 357–366, Aug. 1996.

[7] O. P. Gandhi, G. Lazzi, and C. M. Furse, "Electromagnetic absorption in the human head and neck for mobile telephones at 835 and 1900 MHz," *IEEE Trans. Microwave Theory Tech.*, vol. 44, pp. 1884–1897, Oct. 1996.

[8] M. Okoniewski and M. A. Stuchly, "A study of the handset antenna and human body interaction," *IEEE Trans. Microwave Theory Tech.*, vol. 44, pp. 1855–1864, Oct. 1996.

[9] V. Hombach, K. Meier, M. Burkhardt, E. Kuhn, and N. Kuster, "The dependence of EM energy absorption upon human head modeling at 900 MHz," *IEEE Trans. Microwave Theory Tech.*, vol. 44, pp. 1865–1873, Oct. 1996.

[10] S. Watanabe, M. Taki, T. Nojima, and O. Fujiwara, "Characteristics of the SAR distributions in a head exposed to electromagnetic fields radiated by a hand-held portable radio," *IEEE Trans. Microwave Theory Tech.*, vol. 44, pp. 1874–1883, Oct. 1996.

[11] J. S. Colburn and Y. Rahmat-Samii, "Human proximity effects on circular polarized handset antennas in personal satellite communications," *IEEE Trans. Antennas Propagat.*, vol. 46, pp. 813–820, June 1998.

[12] G. Lazzi and O. P. Gandhi, "On modeling and personal dosimetry of cellular telephone helical antennas with the FDTD code," *IEEE Trans. Antennas Propagat.*, vol. 46, pp. 525–530, Apr. 1998.
[13] M. A. Mangoud, R. A. Abd-Alhameed, and P. S. Excell, "Simulation of human interaction with mobile telephones using hybrid techniques over coupled domains," *IEEE Trans. Microwave Theory Tech.*, vol. 48, pp. 2014–2021, Nov. 2000.
[14] G. Cerri, P. Russo, A. Schiavoni, G. Tribellini, and P. Bielli, "A new MoM-FDTD hybrid technique for the analysis of scattering problems," *Electron. Lett.*, vol. 34, pp. 438–439, Mar. 1998.
[15] P. Bernardi, M. Cavagnaro, S. Pisa, and E. Piuzzi, "Evaluation of the power absorbed in a human head model exposed to cellular phones equipped with helical antennas," in *IEEE MTT-S Int. Microwave Symp. Dig.*, Boston, MA, June 2000, pp. 1021–1024.
[16] ——, "A graded-mesh FDTD code for the study of human exposure to cellular phones equipped with helical antennas," *Appl. Comput. Electromag. Soc. J.*, vol. 16, pp. 90–96, Mar. 2001.
[17] J. Wang and O. Fujiwara, "FDTD computation of temperature rise in the human head for portable telephones," *IEEE Trans. Microwave Theory Tech.*, vol. 47, pp. 1528–1534, Aug. 1999.
[18] G. M. J. Van Leeuwen, J. J. Lagendijk, B. J. A. M. Van Leersum, A. P. M. Zwamborn, S. N. Hornsleth, and A. N. T. J. Kotte, "Calculation of change in brain temperatures due to exposure to a mobile phone," *Phys. Med. Biol.*, vol. 44, pp. 2367–2379, 1999.
[19] P. Bernardi, M. Cavagnaro, S. Pisa, and E. Piuzzi, "Specific absorption rate and temperature increases in the head of a cellular-phone user," *IEEE Trans. Microwave Theory Tech.*, vol. 48, pp. 1118–1126, July 2000.
[20] P. A. Mason, J. M. Ziriax, W. D. Hurt, T. J. Walters, K. L. Ryan, D. A. Nelson, K. I. Smith, and J. A. D'Andrea, "Recent advancements in dosimetry measurements and modeling," in *Radio Frequency Radiation Dosimetry*, B. J. Klauenberg and D. Miklavcic, Eds. Norwell, MA: Kluwer, 2000, pp. 141–155.
[21] S. Gabriel, R. W. Lau, and C. Gabriel, "The dielectric properties of biological tissues: III—Parametric models for the dielectric spectrum of tissues," *Phys. Med. Biol.*, vol. 41, pp. 2271–2293, 1996.
[22] C. Gabriel, "Compilation of the dielectric properties of body tissues at RF and microwave frequencies," Brooks Air Force, Brooks AFB, TX, Tech. Rep. AL/OE-TR-1996-0037, 1996.
[23] P. Eratuuli, P. Haapala, and P. Vainikainen, "Dual frequency wire antennas," *Electron. Lett.*, vol. 32, no. 12, pp. 1051–1052, June 1996.
[24] J. Burke and A. Poggio, "Numerical electromagnetics code (NEC)—Method of moments," Lawrence Livermore Nat. Lab., Livermore, CA, Tech. Rep. UCID-18834, 1981.
[25] Q. Balzano, O. Garay, and T. J. Manning, "Electromagnetic energy exposure of simulated users of portable cellular telephones," *IEEE Trans. Veh. Technol.*, vol. 44, pp. 390–403, Aug. 1995.
[26] P. J. Dimbylow and S. M. Mann, "SAR calculations in an anatomically realistic model of the head for mobile communication transceivers at 900 MHz and 1.8 GHz," *Phys. Med. Biol.*, vol. 39, pp. 1537–1553, 1994.
[27] O. P. Gandhi, G. Lazzi, and C. M. Furse, "Electromagnetic absorption in the human head and neck for mobile telephones at 835 and 1900 MHz," *IEEE Trans. Microwave Theory Tech.*, vol. 44, pp. 1884–1897, Oct. 1996.
[28] "Digital cellular telecommunication system, radio transmission and reception," ETSI, Sophia Antipolis, France, Tech. Rep. GSM 05.05, 1996.
[29] ICNIRP, "Guidelines for limiting exposure to time-varying electric, magnetic, and electromagnetic fields (up to 300 GHz)," *Health Phys.*, vol. 74, no. 4, pp. 494–522, 1998.
[30] "Council recommendation on limits for exposure of the general public to electromagnetic fields: 0 Hz–300 GHz," Commission Eur. Communities, Brussels, Belgium, June 1998.
[31] *IEEE Standard for Safety Levels with Respect to Human Exposure to Radio Frequency Electromagnetic Fields, 3 kHz to 300 GHz*, IEEE Standard C95.1, 1999.
[32] "Evaluating compliance with FCC guidelines for human exposure to radio-frequency electromagnetic fields," FCC, Washington, DC, OET Bull. 65, Aug. 1997.
[33] N. Ozisik, *Heat Transfer: A Basic Approach*. New York: McGraw-Hill, 1985.
[34] A. C. Guyton, *Textbook of Medical Physiology*. Philadelphia, PA: Saunders, 1991.
[35] J. Wiart, C. Dale, A. V. Bosisio, and A. Le Cornec, "Analysis of the influence of the power control and discontinuous transmission on RF exposure with GSM mobile phones," *IEEE Trans. Electromagn. Compat.*, vol. 42, pp. 376–385, Nov. 2000.

Paolo Bernardi (M'66–SM'73–F'93) was born in Civitavecchia, Italy, in 1936. He received the Electrical Engineering and Libera Docenza degrees from the University of Rome, Rome, Italy, in 1960 and 1968, respectively.

Since 1961, he has been with the Department of Electronics, University "La Sapienza" of Rome, Rome, Italy, where he became a Full Professor in 1976 and was Director of this department from 1982 to 1988. His research has dealt with the propagation of EM waves inferrites, microwave components, biological effects of EM waves, and EM compatibility. He has authored over 150 scientific papers and numerous invited presentations at international workshops and conferences. He was an Associate Editor for the *URSI Radio Science Bulletin*. He is on the Editorial Board for *Microwave and Optical Technology Letters*. He was the guest editor of special issues on "Nonionizing Electromagnetic Radiation" of *Alta Frequenza* (Mar. 1980) and "Exposure Hazards and Health Protection in Personal Communication Services" of *Wireless Networks* (Dec. 1997).

Dr. Bernardi is a member of the Bioelectromagnetics Society (BEMS), European Bioelectromagnetics Association (EBEA), and "Socio Fedele" of the Italian Electrical and Electronic Society (AEI). From 1979 to 1980, he was the chairman of the IEEE Middle and South Italy Section. He was chairman of the URSI Commission K on Electromagnetics in Biology and Medicine (1993–1996), vice-chairman of the European Community COST Project 244 on Biomedical Effects of Electromagnetic Radiation (1993–1997), and project coordinator of the European Community Project CEPHOS (1998–2000), which was devoted to EM dosimetry and compliance with standards of mobile cellular phones. He is currently the scientific coordinator of the Italian national project (2001–2003), which is devoted to the protection of people and environment from EM emissions. He is an Editorial Board member for the IEEE TRANSACTIONS ON MICROWAVE THEORY AND TECHNIQUES. He was the recipient of the 1984 IEEE Centennial Medal.

Marta Cavagnaro was born in Rome, Italy, in 1966. She received the Electronic Engineering degree (*cum laude*) and the Ph.D. degree from the University "La Sapienza" of Rome, Rome, Italy, in 1993 and 1997, respectively.

She is currently with the Department of Electronic Engineering, University "La Sapienza" of Rome, where she is an Assistant Professor. Her current research interests are dosimetric aspects of the interaction between EM fields and biological systems and numerical techniques.

Dr. Cavagnaro was the recipient of the 1996 URSI Young Scientist Award.

Stefano Pisa (M'91) was born in Rome, Italy, in 1957. He received the Electronic Engineering and Ph.D. degrees from the University "La Sapienza" of Rome, Rome, Italy, in 1985 and 1988, respectively.

He is currently a Researcher with the Department of Electronic Engineering, University "La Sapienza" of Rome. His research interests are in the interaction between EM fields and biological systems and therapeutic and diagnostic applications of EM fields.

Emanuele Piuzzi was born in Galatina, Lecce, Italy, in 1972. He received the Electronic Engineering degree (*cum laude*) and the Ph.D. degree from the University "La Sapienza" of Rome, Rome, Italy, in 1997 and 2001, respectively.

He is currently studying hybrid techniques for the solution of Maxwell's equations and thermal models for the human body under EM-field exposure. His main research interests are related to the study of the interaction between EM fields radiated by mobile communication systems and exposed subjects, and of therapeutic applications of EM fields (microwave tissue ablation). He is also interested in smart antennas for cellular base stations and in low-SAR antennas for cellular handsets.

Dr. Piuzzi was the recipient of one of the 1999 URSI Young Scientist Awards.